Bose-Einstein statistical properties and condensation of excitonic molecules in CuCl

N. Peyghambarian* and L. L. Chase
Physics Department, Indiana University, Bloomington, Indiana 47405

A. Mysyrowicz
Group de Physique des Solides, Ecole Normale Superieure, Université Paris VII, Tour 23, F-75005 Paris, France

(Received 19 August 1982; revised manuscript received 10 November 1982)

A comprehensive investigation of the optical properties of excitonic molecules in CuCl films is presented and discussed. The experimental work includes resonant two-photon absorption (TPA), observations of the resonantly excited biexciton emission, and optical pump-and-probe studies. The collision broadening of the TPA implies a collision rate $\sim 10^{-12}$ sec for the biexcitons, which is sufficiently rapid to establish a quasithermal equilibrium for the particles on a time scale that is short in comparison with the biexciton lifetime and the duration of the laser pump pulse. The biexciton luminescence line shapes obtained with resonant $\vec{k}=0$ two-photon excitation have been fitted using a Bose-Einstein thermal distribution of biexcitons. The chemical potential obtained from the fits goes to zero as the biexciton density is increased at a fixed lattice temperature or if the lattice temperature is decreased at fixed density. The sharp luminescence features that are observed at high densities and low temperatures with single-beam, two-photon excitation are interpreted as resulting from a Bose-Einstein—condensed state of the biexcitons at twice the wave vector of the laser pumping photons. Further evidence for a condensed state is obtained from optical-probe measurements in which a small number of probe biexcitons is injected into the sample, with and without the presence of a condensed state produced by an intense laser pump beam. The luminescence of these injected probe biexcitons is modified in the presence of the pump beam such that it exhibits the sharp features of the emission from the condensed state. Measurements of optical gain and stimulated emission in the presence of the pump beam show that the redistribution of the probe luminescence does not result from those processes, but must involve a preferential redistribution of the probe particles in momentum space via collisions. Such a redistribution is expected when additional particles are added to a condensed system of bosons.

I. INTRODUCTION

In a number of wide-band-gap semiconductors, optical absorption, and luminescence studies have confirmed the existence of the free biexciton (or excitonic molecule) in the range of intermediate to high excitation levels.[1] The most extensive work has been carried out on the direct-band-gap material CuCl in which the biexciton has several remarkable properties which suggest the possibility of observing Bose-Einstein statistical behavior of these particles at high densities and low temperatures.[2] The binding energy of the CuCl biexciton is about 26 meV relative to the lowest exciton state, and it is therefore stable up to temperatures on the order of 100 K. Its radius can be estimated from recent theoretical results[3] to be about 10—15 Å; this implies that biexciton densities on the order of 10^{19} cm^{-3} might be achieved without affecting the stability of these quasiparticles. Recent measurements of the effective mass of the Z_3 exciton[4] yield an effective mass for the biexciton of about 5.3 free-electron masses, making it a rather light particle.

Despite their rather short lifetime of $\sim 10^{-9}$ sec, it has been possible to produce biexciton densities in the $(10^{18}$—$10^{19})$-cm^{-3} range by pulsed-laser excitation, either indirectly using band-to-band or free-exciton absorption, or by direct excitation of specific wave-vector states using resonant two-photon absorption.[1] For a particle density $n \sim 10^{19}$ cm^{-3}, a Bose-Einstein condensation (BEC) temperature of 25 K for biexcitons in CuCl can be estimated from the formula appropriate to an ideal Bose gas,[5]

$$T_c = \frac{h^2}{2\pi M k_B}\left[\frac{n}{2.612}\right]^{2/3},$$

where M is the mass of the particles. This expres-

sion provides a fairly accurate prediction of $T_c = 3.14$ K (Ref. 5) for the superfluid transition in liquid ^{4}He in which the effects of interparticle interactions are large. It should also provide a reasonable estimate of T_c for a gas of excitonic particles that may, in principle, approach much more closely the properties of ideal bosons than ^{4}He.

Most of the theoretical work concerning biexciton properties and the possibility of BEC has been reviewed and discussed recently by Hanamura and Haug.[1] Calculations for biexcitons in CuCl in the Boguliubov approximation show that at a density of 10^{19} cm^{-3}, 65% of the total molecules would be in the condensed state for $T \ll T_c$. Biexcitons in CuCl have the very useful property that the luminescence arising from their optical decay can be used as a probe of their energy distribution. The luminescence spectrum calculated for the condensed phase (neglecting the polariton dispersion of the final exciton states in the transition) shows a broad sideband from the uncondensed particles, in addition to sharp emission lines from the condensed state.[1] The width and intensity of the sideband are determined by interactions between the particles and depend on the particle density. The width of the sharp line is influenced by collisions of the exciton in the final state. It will be shown later, however, that the inclusion of the polariton effects for the final exciton state leads to the conclusion that no sharp emission line from the condensate should be observed if BEC occurs exactly at $\vec{k}=0$.

Hanamura and Inoue[6] have studied theoretically the dynamics of BEC taking various initial conditions for the population of biexcitons at $T=0$ and considering thermalization via biexciton-phonon interactions. They found that the time required for BEC to occur is comparable with, or longer than, the biexciton lifetime, so that BEC may be impossible under normal circumstances. Recently Yakhot and Levich[7] have considered the possibility of a nonequilibrium condensation of biexcitons nucleated by the resonant laser pumping. They showed that the time for BEC to occur is considerably shortened if interparticle collisions are taken into account, since the initial pumped state acts as a nucleation center. An interesting aspect of this type of condensation, in which the kinetics of the condensation process result from particle collisions rather than phonons, is that the condensation occurs at the wave vector of resonant excitation.

With regard to the experimental problem of searching for nonclassical statistical behavior of excitons and biexcitons, it is possible to create either initial "hot"- or "cold"-biexciton distributions by different modes of laser excitation and to observe the resulting steady-state or time-dependent energy distributions of the biexcitons through analysis of their luminescence as their density and temperature are varied. As the temperature is lowered from above T_c at a fixed particle density, or as the density is increased at a fixed temperature by increasing the rate of laser excitation, the energy distribution should change from a Maxwell-Boltzmann distribution to a Bose-Einstein distribution with a finite chemical potential that approaches zero at T_c. An actual condensation in momentum space would be indicated by the appearance of a "spike" at $\vec{k}\sim 0$ in the momentum distribution either below a threshold temperature T_c or above a threshold density of particles. These features would appear at first sight to be unambiguous indications of quantum-statistical behavior. There are, however, experimental problems connected with such a straightforward interpretation of luminescence results, and a brief review of the previous spectroscopic results reported for biexcitons in CuCl is therefore appropriate.

There have been numerous studies of luminescence, hyper-Raman scattering, and two-photon absorption involving biexcitons in CuCl. In the earliest studies of the optical-emission spectra of biexcitons produced at twice the wave vector of the incident light by resonant two-photon absorption sharp emission components were reported that decreased rapidly in intensity above 30—40 K, and they were attributed to BEC of the biexcitons.[8,9] In addition, sharp emission components were observed that shifted in frequency as the frequency of the exciting laser was changed, and these were attributed to a resonant hyper-Raman scattering process in which two laser photons excite a virtual biexciton and one photon is reemitted leaving an exciton-polariton in the crystal.[10] Much work has been performed subsequently with more monochromatic laser sources and faster excitation pulses. It has been argued by various authors that the sharp luminescence features which are observed with resonant excitation result either from the hyper-Raman scattering or from a "cold gas" of biexcitons[11–13] that radiatively decay before undergoing thermalizing collisions with phonons or thermalized excitonic particles. This ambiguity could be avoided if the biexcitons could be produced by nonresonant excitation at high enough densities and low enough temperatures for condensation to occur. Luminescence spectra obtained by laser pumping into the exciton and electron-hole continuum regions have been measured and fitted to classical thermal biexciton distributions.[9,14] The effective particle temperatures observed with nonresonant pumping are higher than the lattice temperature because of the excess of 30 meV or more per biexciton that must be given up to the lattice. No evidence has been reported as yet for

nonclassical behavior of nonresonantly excited biexcitons.

A complication in interpreting biexciton luminescence data arises from its large radiative decay rate, estimated to be 10^8–10^9 $\sec^{-1}$.[15] Optical gain and stimulated emission associated with the biexciton emission have been measured under conditions of both resonant[16,17] and nonresonant[18,19] excitation. At the biexciton densities of interest in searching for Bose-Einstein statistical behavior, the gain is large enough to cause severe distortions of the intensity distribution of the luminescence[16] if care is not taken to minimize the effects of stimulated emission. It is also possible that stimulated emission may lead to threshold effects in the intensities of the sharp emission components that would otherwise be evidence for BEC.

Recently, the present authors reported on the luminescence of biexcitons produced by resonant excitation at $\vec{k}=0$ and $2\vec{k}_p$, where $k_p=4.44\times10^5$ cm^{-1} is the photon wave vector in thin films of CuCl.[20] Sharp polarized luminescence components having spatially anisotropic intensity distributions developed when the laser excitation at $2\vec{k}_p$ increased above a temperature-dependent threshold. The threshold behavior and anisotropy of these lines and the absence of a Raman-type shift when the frequency of the pump laser was varied implied that neither cold-gas emission nor the hyper-Raman process can account for them. With $\vec{k}=0$ excitation, the sharp features were not present because of the selection rules governing the optical decay and the large wave-vector dependence of the polariton branches near $\vec{k}=0$. The substantial changes that were observed with increasing $\vec{k}=0$ excitation intensity were, however, qualitatively similar to those expected for the transition from a classical Boltzmann distribution to a Bose-Einstein distribution with a chemical potential μ approaching zero. It was stated that these features provided substantial evidence for the presence of BEC of the biexcitons.[20]

Sôtome *et al.*[21] subsequently studied the emission spectrum of biexcitons excited at $2\vec{k}_p$ in CuCl films and concluded that the sharp components are due to hyper-Raman scattering. They argued that random strain broadening of the biexciton state in some samples was responsible for the absence of a shift of the sharp line when the laser frequency was varied. Kushida,[22] on the other hand, suggested that the sharp lines might arise from cold-gas emission, and that the redistribution of the emission produced by $\vec{k}=0$ excitation results from stimulated emission.

It should be clear from even this brief history of the biexciton in CuCl, as well as the search for BEC of excitonic particles in some other semiconductors, that the observation of changes in luminescence distribution alone will not be sufficient to establish the existence of BEC. This is particularly true in the case of resonant laser excitation of a single band of biexciton or exciton states. The laser excitation itself imparts coherence to the system. If it can be shown that this coherence is destroyed rapidly by collisions or other scattering processes at low densities or high temperatures, but the coherence is stable at high particle densities and low temperatures, as we argued in our earlier Letter,[20] then this might be taken as evidence of a nonequilibrium condensed state along the lines of Ref. 7, even if it is not an actual condensation from an initial thermal distribution. Evidence of a more direct nature, however, would involve showing convincingly that the uncondensed part of the biexciton distribution corresponds to a Bose-Einstein distribution and/or that additional particles added to the system at other places in momentum space are preferentially attracted to the condensed state. It is the purpose of the present paper to demonstrate these properties for biexcitons in CuCl.

Although we have also studied the biexciton emission in single-crystal CuCl, all of the results that will be presented in this paper have been obtained on evaporated and annealed thin films. The use of such very thin samples allows the best spatial uniformity of the optically pumped biexciton density. In addition, the small dimensions of the excited region minimize the effects of stimulated emission at the large biexciton densities required for BEC to occur.

II. EXPERIMENTAL PROCEDURES

The films of CuCl that were used in this work were prepared by evaporating high-purity bulk single crystals onto fused-quartz substrates at pressures $\sim10^{-7}$ Torr. The substrates were held at 120°C during evaporation and for a subsequent annealing period of about 4 h. In most cases, the films were immediately mounted on the cold finger of a cryostat, which was then evacuated. Prior to thermal cycling of the films, microscopic observation showed no visible breaks or defects in the films. After cycling to 4.2 K and back to room temperature, however, a network of very thin cracks with a spacing of 50 μm to several hundred micrometers was formed by the differential contraction of the film and substrate. It is likely that most of the thermal stress in the films was relieved in this way since the biexciton and exciton energies were quite reproducible and within ~0.2 meV of the values obtained in single crystals of CuCl. The linewidth of the biexciton two-photon absorption was no more

than a factor of 2 larger than the best values reported for single-crystal platelets of CuCl,[23] and in some films linewidths identical to those in single crystals were observed. The thicknesses of the films, which were typically in the range 1—4.5 μm, were controlled during evaporation by a quartz-thickness monitor.

The samples were mounted onto the cold finger of a variable-flow liquid-helium cryostat with a pinhole ranging in diameter from 5—100 μm in immediate contact with the film. The pinholes facilitated the alignment and precise overlap of the multiple laser beams and, more importantly, also limited the excited volume to regions with maximum dimensions as small as a few micrometers. Although the pinholes reduce the total luminescence at a given laser-pump intensity, we found it very important to reduce the size of the excited region to minimize the effects of stimulated emission for all directions of propagation in the film.

The best and most reproducible experimental results were obtained with fresh samples. Broader biexciton luminescence and stronger bound-exciton luminescence and absorption were observed in films that had been stored for extended periods or repeatedly cycled in temperature. The frequent changes of sample made it impossible to obtain a complete set of data on one sample, but the basic features of the experimental results did not vary substantially from one sample to another.

Two N_2 laser-pumped tunable dye lasers of the Hänsch design[24] were used in these experiments. Both lasers had intracavity-beam-expansion optics to narrow the linewidths to <0.1 Å (0.08 meV for one laser and ~ 0.1 Å for the other). The laser-pulse duration was 4.5 nsec. Induced absorption and optical-gain measurements were performed using the broad luminescence of a pumped dye cell as a probe continuum. The dye laser of narrower linewidth was made to lase at two frequencies simultaneously by placing glass wedges of different wedge angles over two portions of the grating reflector of the cavity.[25] The difference in the wavelengths of the two lasing outputs was continuously adjustable by rotations of the wedges. Thus three frequencies were available for the probe measurements described in Sec. IV C.

Luminescence and absorption spectra were obtained by use of a 0.75-m scanning monochromator in various grating orders, with a resolution as low as 0.1 Å. Spectra were recorded using either a photomultiplier tube and gated integrator in the scanning mode or by replacing the output slit of the monochromator with an intensified semiconductor-diode—array detector. In the latter mode of operation the best resolution was ~ 0.25 Å.

III. PROPERTIES OF EXCITONS AND BIEXCITONS IN CuCl

The lowest-energy exciton states in CuCl are derived from a hole in the upper Γ_7 valence band and an electron in the Γ_6 conduction band. These are a Γ_2 exciton and a Γ_5 exciton that is higher in energy because of the electron-hole exchange interaction.[26] The Γ_2 exciton is optically inactive. The Γ_5 state interacts strongly with the electromagnetic field and is split into longitudinal and transverse branches separated by 5.7 meV at $\vec{k}=0$, as shown in Fig. 1. The Γ_2 exciton is at about 3.199 eV at 4 K. The lowest biexciton level is a totally symmetric state of spin-paired electrons and holes with a total energy at $\vec{k}=0$ of 6.372 eV, or 3.186 eV per electron-hole pair.

The dispersion curves of the Γ_5 excitons and the biexciton have been quite extensively investigated by means of the hyper-Raman scattering process.[27,28] The most extensive measurements[28] extend out to nearly 10% of the Brillouin-zone-boundary wave vector and are well fitted by a polariton-dispersion model that can be used in fitting biexciton-luminescence data to thermal statistical distributions in Secs. IV B and IV C.

IV. EXPERIMENTAL RESULTS

Three types of experiments have been performed on biexcitons in CuCl films: (1) two-photon absorp-

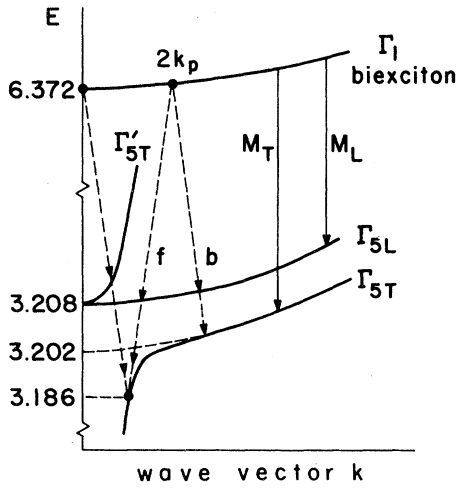

FIG. 1. Schematic dispersion curves of the biexciton Γ_5 exciton branches in CuCl. Dashed lines labeled f and b represent the biexciton decay from $2\vec{k}_p$ with the emission of a photon in the forward and backward directions, respectively. Decays labeled M_T and M_L are from the thermal distribution of biexcitons, which have average wave vectors much larger than $2\vec{k}_p$ for $T \gtrsim 5$ K. Note that the decay from $k=0$ to $\Gamma_{5,L}$ is symmetry forbidden, and the decay to $\Gamma'_{5,T}$ is expected to be very weak.

tion and excitation spectra, (2) luminescence under various conditions of laser excitation, and (3) optical-probe and -gain measurements. The results obtained in each of these experiments yield evidence in support of Bose-Einstein statistical properties and condensation of the biexcitons.

A. Two-photon absorption

The biexciton can be created directly by two-photon absorption (TPA) at wave vectors in the range from zero to $2\vec{k}_p$, where $\vec{k}_p$ is the photon wave vector. Measurements have been performed on thin-film samples using either a one-beam geometry, leading to biexcitons at $2\vec{k}_p$, or a two-beam geometry in which one photon is absorbed from each beam to create a $\vec{k}\sim 0$ biexciton. The thin-film samples are ideal for the study of the TPA because the fraction of incident light absorbed at the peak of the TPA remains much smaller than unity over the entire range of incident power levels of interest in this study. The importance of this feature can be illustrated by considering the general expression for I_t/I_0, the fraction of a single light beam transmitted through a sample of thickness l in the presence of both two-photon absorption and a background linear-absorption coefficient α,[29,30]

$$\frac{I_t}{I_0}=\frac{(1-R_1)(1-R_2)e^{-\alpha l}}{1+N\gamma_2 I_0(1-R_1)(1-e^{-\alpha l})/\alpha}\ . \tag{1}$$

Here N is the number of unit cells per unit volume, γ_2 is the TPA absorption cross section, and R_1 and R_2 are the reflectivities of the entrance and exit surfaces of the film and substrate. If the second term in the denominator is small compared with unity, Eq. (1) may be approximated by

$$\frac{I_t}{I_0}\cong(1-R_1)(1-R_2)e^{-\alpha l}\times[1-N\gamma_2 I_0(1-R_1)(1-e^{-\alpha l})/\alpha]\ . \tag{2}$$

This implies that the TPA absorption dip will have a profile as a function of laser frequency that is proportional to γ_2 and I_0. However, γ_2 is intensity dependent because of collision broadening of the biexciton state so that Eq. (1) is not exact in our case at high intensity. In our measurements, the second term in the brackets in Eq. (2) is less than 0.25 at the peak of the TPA, so the measured TPA profile is as close to the true frequency dependence of γ_2 as possible, considering this problem.

The Γ_1 symmetry of the ground state of the biexciton imposes selection rules on the one- and two-beam TPA process.[31] We have found these selection rules to be well obeyed in the thin films at low power levels ($\ll 1$ MW/cm^2). The TPA disappears with opposite circular or opposite linear polarizations of two counterpropagating laser beams. The single-beam TPA polarization has also been examined, and it is found that the transition is allowed in linear polarization but forbidden in circular polarization. Both the one- and two-beam polarization dependences of the TPA are in agreement with the selection rules for excitation of the totally symmetric biexciton level.[31] At power levels exceeding about 1 MW/cm^2, there are large deviations from these selection rules. These deviations possibly result from nonlinear interactions between the polaritons in the CuCl leading to depolarization of the laser beams.[32]

The linewidth of the TPA at the lowest intensities is somewhat sample dependent; it is as low as 0.15 Å (0.12 meV) or less in some samples and averages 0.25 Å (0.2 meV) in the various samples used. This average width corresponds to a width of 0.4 meV for the biexciton state, less than a factor of 2 larger than the lowest width reported in single crystals.[33] It should be noted that the transmission of the sample goes to zero at higher photon energies in the region of the strong Γ_5 exciton absorption, which shows that these results are not affected by light leakage through gaps or irregularities in the films.

At moderate incident intensities ($\lesssim 1$ MW/cm^2) the TPA displays a marked symmetric broadening with increasing laser intensity. The origin of this broadening has been the source of some controversy recently. We[30] and others[34] have attributed this effect to collisions among the biexcitons and excitons produced by the laser excitation. This interpretation is supported by a more recent experiment in which the $\vec{k}\cong 0$ TPA, measured with two weak beams of different frequencies, is broadened by the simultaneous pumping of biexcitons at $\vec{k}=2\vec{k}_p$ by a single intense beam.[35] It is possible that a contrary result obtained by Kuwata *et al.*[36] can be attributed to a nonuniform excitation over the thickness of a platelet sample. The fact that the transmission at the center of the TPA remains close to unity in the films used in our measurements rules out the recent claim[37] that the broadening merely results from the nonlinear dependence of I_t/I_0 on $\gamma_2(\omega)$ in Eq. (1) in the limit where $I_t/I_0\to 0$ at the resonance center.

In the presence of collisional broadening caused by excitonic particles generated by the TPA, the TPA line shape must be calculated self-consistently for a particular collision model. Such a calculation has been done[30] for the case of liquidlike collisions in which the scattering rate is proportional to the ratio of the mean thermal velocity to the interparticle separation. The result is a nearly Lorentzian line shape, although one with reduced absorption far from the peak absorption frequency. The linewidth

in this model is predicted to increases as $I^{1/2}$ and the absorbed power at the peak of the TPA increases as $I^{3/2}$. The observation of a symmetric broadening of the TPA around a unique center frequency and a set of line shapes fitted with Lorentzians as a function of laser intensity have been presented elsewhere.[30] A width increasing in proportion to $I^{1/2}$ has been observed over more than a factor of 10 in laser intensity I, in agreement with these predictions. At intensities higher than a few MW/cm^2, the TPA line shape becomes skewed to higher energy. This effect is not fully understood at present.

Of most importance to the possibility of BEC of the biexcitons is the fact that the linewidths obtained from these fits correspond to a scattering rate for the biexcitons that approaches 10^{12} sec^{-1} at the highest intensities used here. This rate implies that the biexciton distribution will approach a quasiequilibrium thermal distribution, possibly at an effective temperature larger than that of the CuCl lattice, in a time much shorter than the biexciton lifetime and the 4.5-nsec width of the excitation pulse. Considering the rather weak dependence of the width on laser intensity, this situation should remain true for the entire range of intensities used in the present work.

B. Biexciton luminescence

The optical emission resulting from either the radiative decay of the biexciton, or from the resonant hyper-Raman scattering in which the biexciton is the intermediate state, has been extensively studied in single-crystal samples of CuCl. The published results have varied considerably because such factors as the excitation intensity, excitation length, detection geometry, sample condition, and excitation bandwidth are all of importance in determining the qualitative character of the observed spectra. It is quite likely that stimulated emission is responsible for much of this variability. In order to minimize such effects, the data presented here were obtained at power densities close to the threshold of appearance of features indicative of Bose-Einstein statistical properties of the biexcitons. Also, as mentioned before, the dimensions of the excitation spot were held to a minimum consistent with a reasonable signal-to-noise ratio, and care was exercised to ensure that the observed emission originated from the excitation region only, and not from sample edges or imperfections.

The general features of the biexciton luminescence can be illustrated with reference to Fig. 1. In the luminescence decay process a photon is emitted, and either a transverse or longitudinal exciton remains. Thus two bands labeled M_T and M_L in Fig. 1 are observed in the luminescence. Because the effective mass of the biexciton is larger than the masses of the longitudinal and transverse excitons by about a factor of 2, it is clear that the energy of the emitted photon will decrease as the center-of-mass kinetic energy of the biexciton increases. This is the feature that is exploited in order to obtain information about the energy distribution of the biexcitons. For a classical thermal distribution with a mean thermal wave vector much larger than the wave vector of the emitted photon, the momentum of the photon may be ignored. Then it can be shown that the frequency distribution of the emitted light from the decay to each exciton branch has the shape of an inverted Maxwellian,[1]

$$I(\omega)=cE^{1/2}\exp(-E/k_BT_{\text{eff}}) ,$$

with (3)

$$E=(m_B/m_X-1)[E_B(0)-E_X(0)-\hbar\omega] ,$$

where c is a constant, T_{eff} is the effective particle temperature, m_B and m_X are the biexciton and exciton masses, respectively, and $E_B(0)$ and $E_X(0)$ are the energies of the biexciton and exciton states at $\vec{k}=0$. However, Eq. (3) is only an approximation which becomes completely inadequate for biexciton wave vectors comparable to $\vec{k}_p$ because of the polariton structure of the transverse exciton. Since these small wave vectors are of obvious importance in the present study of BEC, the data have been fitted to numerical calculations using the general expression

$$I(\omega)=c\int d^3k_i\int d^3k_f f(\vec{k}_i)\,|M_{if}(\vec{k}_i,\vec{k}_f)|^2 \times\delta(E_i-E_f-\hbar\omega)\delta(\vec{k}_i-\vec{k}_f-\vec{k}_p) , \quad (4)$$

where $f(\vec{k}_i)$ is the distribution function for the biexcitons of wave vector $\vec{k}_i$, $\vec{k}_f$ is the wave vector of the remaining exciton, E_i and E_f are the initial (biexciton) and final (exciton) energies, respectively, and M_{if} is the matrix element for the transition. M_{if} is obtained from the polarization selection rule for the excitation or decay of the totally symmetric biexciton state, $M_{if}^2\propto|\hat{\epsilon}_p\cdot\hat{e}_X|^2$, where $\hat{\epsilon}_p$ and $\hat{e}_X$ are the polarization vectors of the photon and exciton. M_{if}^2 is given by[38]

$$M_{if}^2=|A(\omega)|^2\sin^2\phi \quad (5a)$$

for the decay to a $\Gamma_{5,L}$ exciton, and

$$M_{if}^2=|A(\omega)B(\vec{k}_f)+B(\omega)A(\vec{k}_f)|^2(1+\cos^2\phi) \quad (5b)$$

for the decay to the upper or lower branches of the $\Gamma_{5,T}$ exciton. In these expressions ϕ is the angle be-

tween the wave vectors of the emitted photon and the remaining exciton and is given by

$$\sin^2\phi=\frac{k_i^2\sin^2\theta}{k_i^2+k_p^2-2k_ik_p\cos\theta}\ , \tag{6}$$

where θ is the angle between the biexciton and emitted-photon wave vectors. The A and B coefficients are the photon and exciton parts, respectively, of the emitted photon, or of the remaining transverse polariton in the case of emission to the $\Gamma_{5,T}$ branch[39]

$$A(\mathscr{E})=(1-\mathscr{E}^2)\left[\frac{\left[1+\frac{4\pi\beta}{1-\mathscr{E}^2}\right]^{1/2}}{(1-\mathscr{E}^2)^2+4\pi\beta}\right]^{1/2}\ , \tag{7a}$$

$$B(\mathscr{E})=\left[\frac{4\pi\beta\mathscr{E}}{(1-\mathscr{E}^2)^2+4\pi\beta}\right]^{1/2}\ , \tag{7b}$$

where $\mathscr{E}=\hbar\omega/E_T$ for a polariton of energy $\hbar\omega$, E_T is the energy of the uncoupled transverse branch, and

$$2\pi\beta=E_L^2(0)/E_T^2(0)-1\ .$$

The longitudinal and uncoupled transverse exciton energies are

$$E_L(k)=E_L(0)+\frac{\hbar^2k^2}{2m_L}\ ,$$

$$E_T(k)=E_T(0)+\frac{\hbar^2k^2}{2m_T}\ ,$$

and the coupled transverse branches are solutions of[39]

$$\epsilon=\frac{\hbar^2c^2k^2}{\epsilon_\infty E^2}=1+\frac{4\pi\beta}{1-(E^2/E_T^2)}\ . \tag{8}$$

The parameters used in the present work were obtained from the most extensive and recent hyper-Raman scattering results[28]: $\epsilon_\infty=5.59$, $m_T=2.3m_0$, $m_L=3.14m_0$, $m_B=5.29m_0$, $E_L(0)=3.2079$ eV, and $E_T(0)=3.2025$ eV. The fits to spectra in the remainder of this section were obtained by numerical integrations of Eq. (4) over the biexciton wave vector $\vec{k}_i$, and the angle θ assuming a Bose-Einstein distribution

$$f(E_i)=\{[\exp(E_i-\mu)/k_BT_{\rm eff}]-1\}^{-1}$$

for the biexcitons.

Two different types of excitation were used, either two-photon resonant absorption of a single beam ($2\vec{k}_p$ geometry) or TPA with two counterpropagating beams ($\vec{k}=0$ geometry). In all figures there is a diagram which shows the detection and excitation geometries. All of the luminescence spectra were obtained by observing the luminescence from the surfaces of the films. The two geometries allowed with single-beam excitation are therefore those in which the emission is observed through the side of the film opposite to the excitation surface, where the emitted photons travel at a small angle to the incident photons, or through the excitation surface, where the photons propagate nearly antiparallel to the laser photons. Some spectra were taken with the sample surface perpendicular to the laser beam, and the luminescence photons propagated in a small solid angle centered on the axis of laser propagation; these setups are referred to as either "forward" or "backward" detection. A second geometry was used to minimize the scattered laser light reaching the detection system by detecting the emitted photons at an angle of about 90° to the laser beam, which was incident on the sample surface at an angle of 20°–30° to the normal. Because of the large refractive index of CuCl ($n\sim2.75$), the angle between the wave vectors of the laser and luminescence photons was about 20°, for a "nearly forward" geometry and 160° for a "nearly backward" geometry. Thus all the luminescence data reported here are for propagation in directions near to the normal to the film surface and to the axis of propagation of the excitation beam.

1. *Resonant excitation at* $2\vec{k}_p$

The emission spectra observed with resonant single-beam excitation at $\vec{k}=2\vec{k}_p$ have been studied as a function of sample temperature, excitation intensity, laser frequency, polarization, and detection geometry. Some preliminary results were presented briefly elsewhere.[20] Because of the importance of these results to the question of the existence of BEC, we present in this paper more extensive data on certain aspects of the spectra.

The $\vec{k}=2\vec{k}_p$ spectra observed over a large range of laser intensities at a sample temperature of 20 K are shown in Fig. 2. The laser was focused to a diameter of about 50 μm, and I_0, the maximum power density, was a few MW/cm^2. At low-power densities, most of the integrated luminescence is in the broad M_T and M_L bands. However, at the lowest intensities, there is usually also a narrow N_T line observable whose intensity relative to the Maxwellian bands decreases with increasing sample temperature and varies among the many sets of data obtained on numerous samples. At all power densities, all but a small fraction of the observed luminescence disappears when the excitation laser is detuned from resonance. This implies that the broad M_T and M_L bands originate from biexcitons that are originally

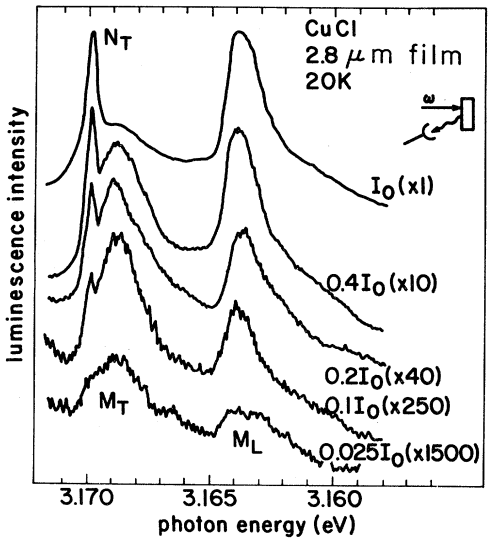

FIG. 2. Biexciton luminescence with one-beam excitation at $2\vec{k}_p$ at $T=20$ K and for a range of laser intensities. $I_0 \sim 1$ MW/cm^2.

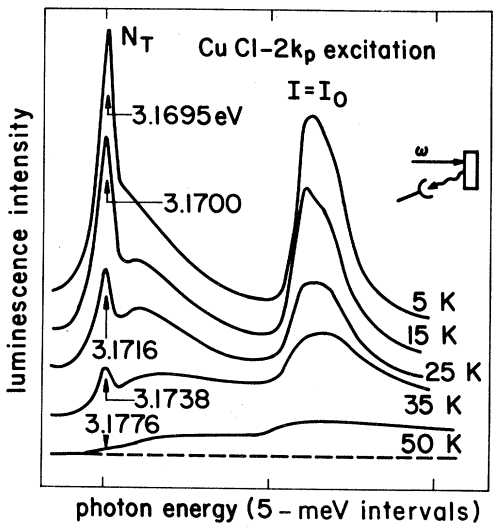

FIG. 3. Biexciton luminescence with single-beam excitation for several temperatures at a laser intensity $I_0 \sim 1$ MW/cm^2. Spectra are shifted so that the N_T lines coincide. Actual energy of the N_T components is indicated at each temperature.

produced at $\vec{k}=2\vec{k}_p$ and are subsequently scattered into a quasithermal distribution. As the excitation intensity is increased an increasing fraction of the luminescence appears in the narrow N_T component and, to a lesser extent, into the narrow N_L component that appears mainly as a sharp shoulder on the M_L band. The low intensity of this N_L line compared with N_T in this geometry results from two factors. The first such factor is the twofold degeneracy of the $\Gamma_{5,T}$ exciton which is the final state for the N_T decay. The $\Gamma_{5,L}$ exciton is nondegenerate. Second, the matrix element in Eqs. (5a) and (6) is proportional to $\sin^2\theta$. For this detection geometry, $160° \lesssim \theta < 180°$ if it is assumed that the biexcitons that contribute to the N_L line are all at or near the $2\vec{k}_p$ pumping wave vector. Further support for this latter assumption is discussed below. At higher excitation levels than those used in Fig. 2, the intensity of the M_L band begins to increase rapidly compared with the other luminescence features. This behavior has also been observed in single crystals of CuCl and was attributed to stimulated emission.[16]

The dependence of the $2\vec{k}_p$ luminescence spectra on sample temperature is illustrated in Figs. 3 and 4 for two excitation intensities. The N_T and N_L components diminish relative to the broad bands as the temperature increases. There is no well-defined threshold for their disappearance, nor is one expected since the laser intensity varies with time and with position in the sample. It is nonetheless clear that the temperature at which the integrated intensity of the N_T line falls below a few percent of the total luminescence intensity is about 40 K for the highest laser intensity, $I=I_0$, and is considerably lower, about 20–25 K, for $I=I_0/10$. A plot of such an arbitrarily defined threshold temperature as a function of laser-power density was presented in an earlier Letter.[20]

The most important question to be addressed in

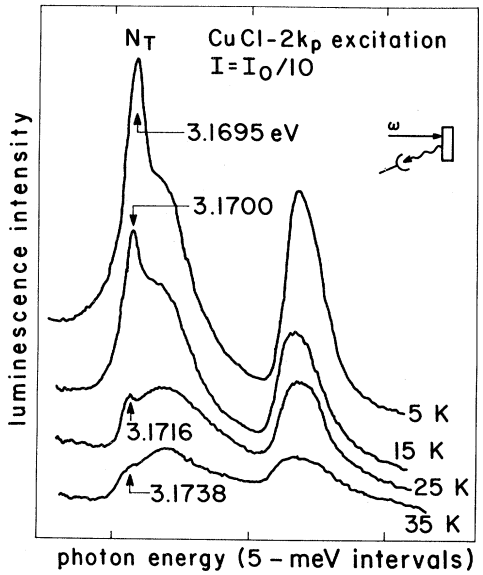

FIG. 4. Biexciton luminescence at several temperatures with single-beam excitation at a laser intensity one-tenth as large as that in Fig. 7.

the context of the present investigation is the nature of the process leading to the sharp N_T and N_L components at low temperatures and high excitation levels. Two further properties of the luminescence spectra that have a bearing on this question are the anisotropy of the luminescence and its dependence on the frequency of the exciting laser. The dependence of the intensities and polarizations of the N_T and N_L lines on the angle between the incident laser photons and the luminescence photons is shown in Fig. 5. The polarization data are corrected for the fresnel coefficients of the film and the polarization characteristics of the detection system by observation of the unpolarized biexciton emission excited by nonresonant pumping. It is therefore clearly associated with the resonantly pumped emission, and not with any effects due to the thin-film geometry as has been suggested by Kushida.[22] There are two features of importance in these spectra. First, the N_T and N_L emission lines are much reduced in intensity for emission in the forward direction (labeled 0° in the figure). In fact, the residual intensity of N_T may be attributed to backward luminescence reflected from the surface of the film, although some emission from an elastically scattered cold-gas component cannot be discounted. Second, the N_L emission line is strongly polarized in the plane of scattering for noncollinear (nearly backward) geometry in which the emitted phonons propagate outside the sample at 90° to the incident laser beam. These results can be accounted for if the N_T and N_L emission lines originate from biexcitons at wave vector $2\vec{k}_p$, at which they are produced. In the forward direction, the N_T emission from $2\vec{k}_p$ must be coincident with the pump-laser energy, i.e., a two-photon reemission. The matrix element for the N_L emission, M_{if}^2 in Eq. (5a), is proportional to the square of the component of the polarization of the emitted photon along the wave vector of the remaining longitudinal exciton. This means that in the noncollinear emission geometry the N_L line must be polarized in the plane of propagation of the pump laser and the emitted photon, and N_L is forbidden in the forward (0°) and backward (180°) emission. In Fig. 5, most of the N_L line disappears in the luminescence polarized perpendicular to this plane. The small residual N_L line in this geometry may result either from light scattered from the thin cracks in the film, or from a deviation from the normal selection rules at high biexciton densities.

The dependence of the biexciton emission spectra on the frequency of the pump laser has been extensively investigated in a number of samples and over a range of excitation intensities. The results are dependent on sample history to some extent and are quite strongly dependent on excitation intensity in the regime where stimulated emission becomes important. The spectra shown in Fig. 6 are typical of

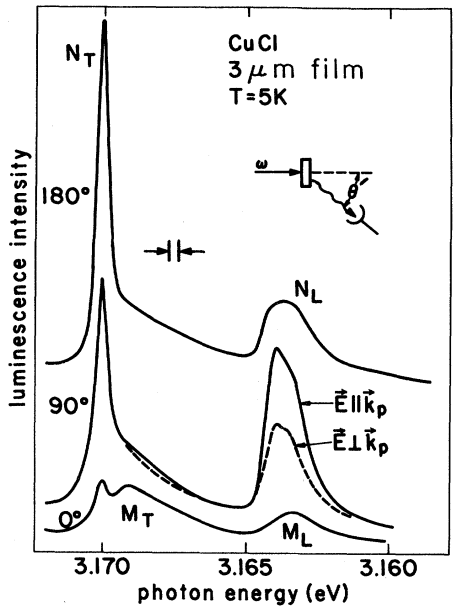

FIG. 5. Anisotropy and polarization of the biexciton luminescence for $2\vec{k}_p$ excitation. Values of θ' shown on the left are the angles of propagation of the emitted photons relative to the direction of the incident laser beam outside the film.

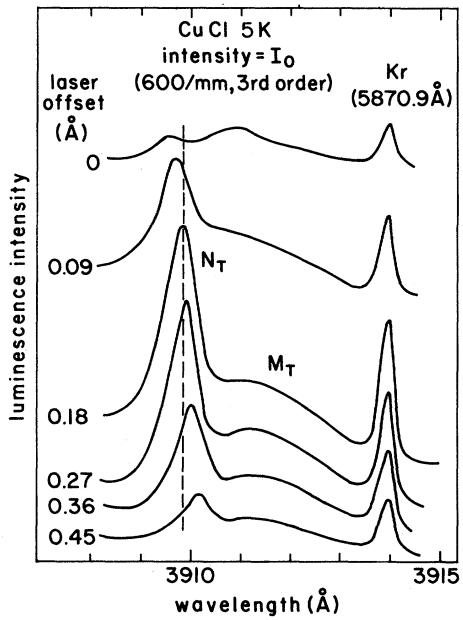

FIG. 6. Biexciton luminescence decay to the Γ_{5T} branch at $T=5$ K as a function of laser excitation wavelength for $2\vec{k}_p$ excitation. Krypton reference line at 5870.9 Å appears in a different grating order.

moderate excitation levels, $I_0 \sim 1$ MW/cm^2, and fresh CuCl films. Only the part of the emission to the transverse branch is shown here since the N_T line is the dominant sharp feature at such intensities. The wavelength shift of the N_T line that is observable in Fig. 6 is about 90% of that of the exciting laser beam. The intensity of the N_T line diminishes rapidly as the laser is detuned from resonance, and it is unobservable when the excitation laser is detuned by one to two halfwidths from the TPA resonance, which corresponds to an offset of about 0.25 Å in Fig. 6. At higher pump intensities, a weak component with a hyper-Raman-type shift, equal to twice the shift of the pump-laser wavelength, is observed for the N_T line. This component remains observable at excitation wavelengths far from the center of the TPA resonance, and its intensity under those circumstances has a marked thresholdlike increase with increasing pump intensity. A plot of the energy and peak intensity of the N_T emission as a function of laser photon energy is shown for two laser intensities in Fig. 7. At the higher laser intensity, a hyper-Raman component is observed only on the high-energy side of the resonance. The fact that this component is not observed at all on the low-energy side suggests that it results from a stimulation process that is inhibited by reabsorption from exciton states populated by the laser pumping when the laser is tuned below the resonance. At still higher excitation intensities, well above 10 MW/cm^2, a very dominant, sharp, and strongly stimulated N_L hyper-Raman line is observed. Typical spectra of this type obtained at a power density of about several tens of MW/cm^2 are shown in Fig. 8. The sharp N_L Raman line should be forbidden in this geometry and is not observable in the optical gain spectra presented in Sec. V. This suggests that it results from stimulated emission in the plane of the film, and is observed by scattering from the cracks in the films. The corresponding N_T component is very much smaller than N_L because of gain saturation due to a buildup of the population of excitons on the lower transverse branch.[16] Such a gain saturation would occur for the N_L line at much higher power levels because of the rapid decay of longitudinal excitons to the lower transverse branch. It is apparent from Fig. 8 that the intensity of the stimulated Raman component has a very sharp threshold behavior as the laser intensity is increased. Near theshold the N_L intensity increases by nearly 2 orders of magnitude when the pump intensity is doubled. At such high excitation levels, the TPA also becomes skewed to higher energies. All of the results presented in this paper were obtained at much lower excitation levels where the total luminescence intensity increased smoothly with pump intensity I, as $I^{1.5}$. This dependence on laser

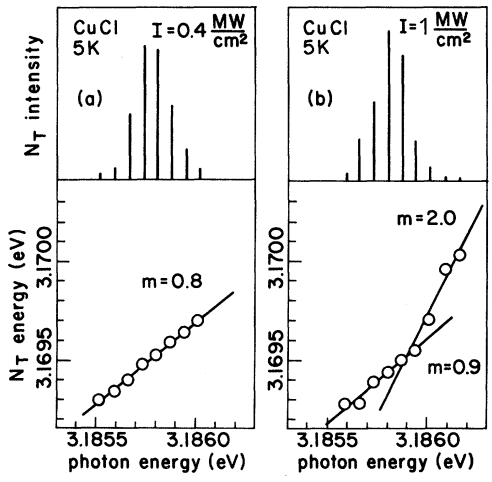

FIG. 7. Photon energy and intensity of the N_T line as a function of the photon energy of the excitation laser for two laser power levels, 0.4 MW/cm^2 in (a) and 1 MW/cm^2 in (b). Radii of the circles around each data point represent the estimated errors in measurement of the photon energies of the laser and the N_T line. Straight lines through the data points yield the slopes m in the relationship $\Delta\nu(N_T) = m\,\Delta\nu$(laser).

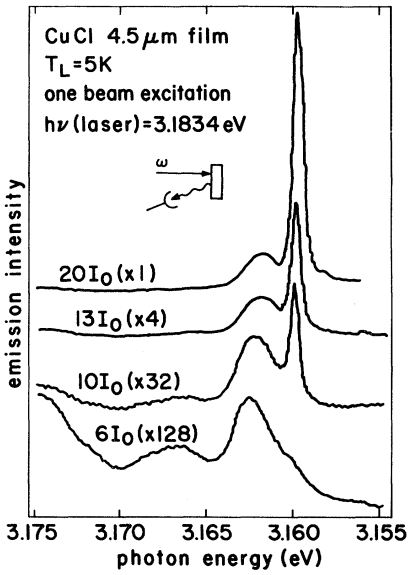

FIG. 8. Biexciton emission spectra at $T=5$ K for $2\vec{k}_p$ excitation with the pump laser tuned about 3 meV to the low-energy side of the TPA resonance. Sharp peak at 3.159 meV has a rapid thresholdlike onset which is indicative of a stimulated Raman decay to the Γ_{5L} branch. Note the large increase in gain of the detection system (given in parentheses) as the laser intensity is reduced by a factor of about 3.

intensity is in agreement with the predictions of the collision-broadening model in Ref. 30.

Sôtome *et al.*[21] have reported data on CuCl films in which they observe substantial shifts of the TPA resonance compared to single crystals, and they also find an additional peak when the laser is tuned off the resonance that they interpret as a phonon-assisted TPA induced by strains in the film. We have not found measurable shifts of the TPA ($\gtrsim 0.5$ Å) in our samples, but we have occasionally observed this additional peak in some samples.

Two possible origins of the sharp emission lines which could account for their intensity and temperature dependence, as well as their anisotropy, are a Bose-Einstein—condensed component of the biexciton distribution at the wave vector of the laser pumping or the stimulated hyper-Raman scattering. A third possibility that has been discussed previously[10,40,41] involves a cold gas of very-low-energy biexcitons which have suffered some sort of dephasing by collisions, but which do not thermalize with other excitonic particles or with the lattice. This possibility can apparently be rejected under the conditions of nearly steady-state excitation used in the present experiments. It is apparent from the anisotropy and polarization data of Fig. 5 that such a cold-gas distribution must be very anisotropic and centered around the pumping wave vector $2\vec{k}_p$. At moderate excitation levels, the emission data of Figs. 2—4 show that most of the emitting particles are in the thermalized distribution, which would coexist with such a cold gas in the steady state, regardless of how the thermalized biexcitons are produced by the resonant pumping. In the absence of quantum attraction due to the Bose nature of the particles any collisions of newly created biexcitons should scatter them predominantly into the thermal distribution, not into some separate cold distribution.

The distinction between stimulated hyper-Raman scattering and BEC at the pump wave vector is difficult to make in a conclusive fashion on the basis of the evidence presented so far. Both processes result from the presence of a coherent biexciton field at $2\vec{k}_p$, so that the anisotropy of the emission would be the same. There is the possibility that stimulated hyper-Raman scattering might account for the increase in the relative intensities of the sharp components with increasing excitation level. However, the Raman components that we have observed at higher excitation intensities, such as those in Fig. 8, have a much more rapid threshold behavior than does the N_T line in Fig. 2.

In principle, the behavior of the sharp lines when the laser is tuned off the TPA resonance peak should provide a basis for distinguishing between luminescence from a condensed state and stimulated hyper-Raman scattering. The small observed shift of the N_T line in Figs. 6 and 7(a) is difficult to account for in terms of Raman scattering. The fact that the N_T component is only observable over a very small range of laser frequencies centered on the TPA resonance, together with the small ratio of the N_T shift to the laser shift, can be accounted for if the residual width of the TPA is due at least partly to an inhomogeneous broadening of the exciton and biexciton levels. This is illustrated in Fig. 9 where it is assumed that the exciton energy in a particular region of the sample is shifted by an amount Δ from the mean value $\tilde{E}_X$. The local biexciton energy would be shifted to the same side of its mean value $\tilde{E}_B$ by 2Δ, since it is reasonable to assume that any inhomogeneous change of the biexciton binding energy would be negligible. It is clear from Fig. 9 that the N_T luminescence frequency ν_E from this region of the sample would shift by the same amount as the shift of the laser frequency, which is close to the observed shift in Fig. 6. On the other hand, an analysis of the effects of such inhomogeneous broadening on the Raman scattering shows that a Raman shift equal to twice the laser shift should occur at least when the laser frequency is tuned beyond the halfwidth of the TPA resonance, and this is not observed. However, the observation of clearly defined stimulated hyper-Raman components at much higher excitation levels still leaves

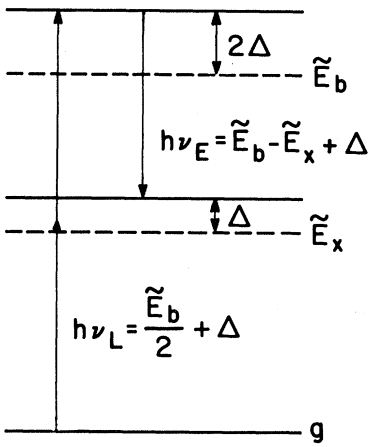

FIG. 9. Schematic energy-level diagram of biexciton and exciton levels for small wave vectors assuming inhomogeneous broadening. $\tilde{E}_B$ and $\tilde{E}_X$ are the most probable energies of the biexciton and exciton states (dashed lines) at $2\vec{k}_p$ and $\sim 3\vec{k}_p$, respectively. Crystal ground state is denoted by g. An assumed shift of the exciton energy in some particular region or regions of the sample is given by Δ. This leads to a shift of 2Δ in the biexciton energy. Resonant TPA and N_T emission photon energies shift by an amount Δ.

some doubt as to how conclusive the data of Figs. 2—6 are in substantiating the origin of the N_T line, even at the lower excitation levels. The results of the probe experiment described in Sec. V are far more convincing in this respect.

2. *Resonant excitation at* $\vec{k}=0$

If biexcitons are produced at or near $\vec{k}=0$ using two counterpropagating laser beams, their direct optical decay is highly constrained by selection rules. Their decay to the lower transverse branch is a two-photon reemission process that recreates the original laser photons, just as was the case for the forward emission from $2\vec{k}_p$. Their decay to the longitudinal branch is forbidden by the selection rule that leads to Eq. (5a), and the matrix element for their decay to the upper transverse branch is expected to be small. Thus no sharp line emission is possible in the region of the M_T and M_L bands. This allows a detailed study to be made of the distribution of thermalized biexcitons as a function of particle density and temperature without the necessity of subtracting intense sharp features from the observed spectra.

Representative data obtained at three temperatures, 5, 25, and 35 K, are shown in Figs. 10—12.

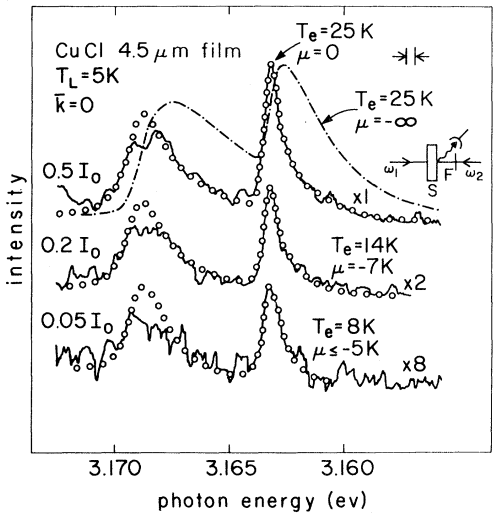

FIG. 10. Luminescence spectra of biexcitons excited at $\vec{k}\sim 0$ at $T_L=5$ K for three laser intensities. Open circles are fits to the data (solid lines) using Eq. (4) with the effective temperature T_{eff} and chemical potential μ given beside each trace. Calculated spectrum for a Maxwell-Boltzmann distribution ($\mu=-\infty$) is shown for the upper trace (dashed-dotted line) using the same values of $T_{\text{eff}}=25$ K as was used for $\mu=0$. Note the intensity scale changes given on the far right of each trace and the laser intensities on the left.

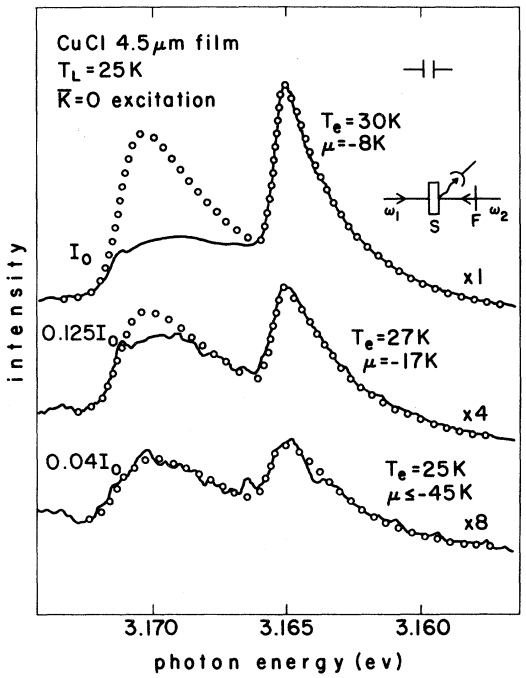

FIG. 11. Same as Fig. 14, only for a lattice temperature $T_L=25$ K.

The biexcitons were produced by two counterpropagating laser beams tuned 2 Å to either side of the TPA so that neither beam could produce biexcitons at $2\vec{k}_p$. The spectra were detected with an intensified-diode array that allowed subtraction of some minor, broad background emission produced independently by each laser beam. A 100-μm pinhole was placed over the sample, and the laser beams were defocused in order to observe the emission from a uniformly illuminated region. The labeled intensities on the left of each spectrum correspond to the intensity of one of the two laser beams,

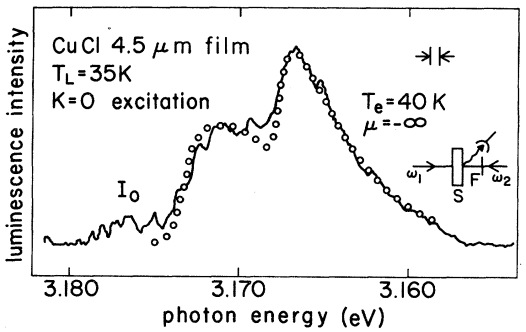

FIG. 12. Same as Fig. 14, only for a lattice temperature $T_L=35$ K. Distribution in this case is indistinguishable from a classical one at all intensities up to the maximum I_0.

which was reduced from the maximum value of $I_0 \sim 1$ MW/cm^2 using neutral density filters. The intensity of the other laser was fixed at a value close to I_0.

The spectrum obtained at each temperature and excitation intensity was fitted to a luminescence distribution calculated by computer using Eq. (4). At $T=5$ K, only the values of the effective particle temperature T_{eff}, the chemical potential μ, and a constant scale factor were variable parameters. At higher temperatures the spectra were shifted by an amount equal to the shift of either the TPA resonance or of the N_T line observed with $\vec{k}=2\vec{k}_P$ excitation at each temperature. A Gaussian broadening was included in the computed distribution to allow for the combined instrumental and intrinsic broadening of the luminescence. The halfwidth of this resolution function was determined from the width of the N_T emission component observed with single-beam excitation.

At each temperature and laser intensity the calculated distribution was fitted to the M_L-band component of the emission, and the values of effective particle temperature T_{eff}, and chemical potential μ so obtained are indicated in the figure. In most cases, the M_T band falls below the calculated distributions to a varying degree dependent on excitation intensity and sample temperature. This is the result of a reabsorption of the M_T light by transverse excitons[42] produced either by decay of the biexcitons or more directly by absorption of the incident laser beams in the tail of the free-exciton line. This effect is particularly pronounced in the relatively thick (4.5-μm) sample used for these measurements in order to obtain the optimum signal-to-noise ratio at the lowest intensities. In a thinner sample, excited by circularly polarized beams of identical frequency, spectra were observed in which both the M_T and M_L bands could be well fitted by a single distribution with $\mu \cong 0$. This is shown in Fig. 13 for sample temperatures of 5 and 25 K. The shift of the M_T band to higher photon energies in the trace for $T=5$ K where $\mu=0$, results from the shift of the biexciton distribution function to lower energies where the final excitons in the optical decay lie on the knee of the transverse exciton branch.

As the excitation intensity increases at each sample temperature, the chemical potential approaches zero, and the effective particle temperature increases because of heating by the optical pumping. A particle density n can be calculated from μ and T_{eff} by integrating over the thermal distribution using the well-known formula

$$n=\frac{2\pi}{h^3}(2M)^{3/2}\int_0^\infty \frac{E^{1/2}}{\exp[(E-\mu)/k_BT]-1}dE \, . \tag{9}$$

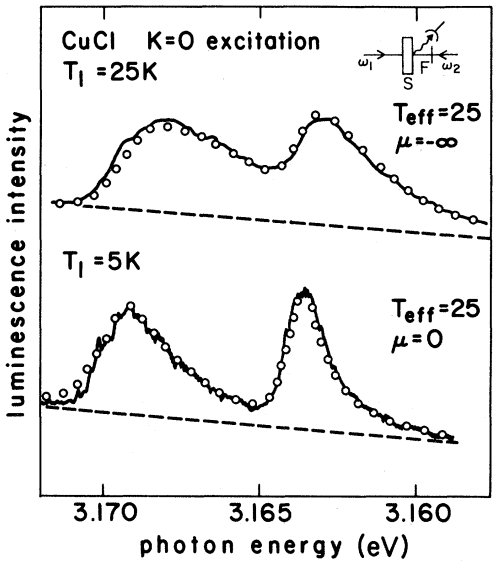

FIG. 13. $\vec{k}=0$ biexciton emission at $T=25$ and 5 K for a sample and excitation conditions in which reabsorption of the M_T band was minimal. Open circles are fits to the spectra using Eq. (4). The upper trace was taken at a much lower laser power density than the lower trace.

These calculated particle densities increase monotonically, although in a sublinear fashion, with the intensity of the attenuated laser beam. Such a sublinear behavior is not particularly surprising since the increase in the TPA linewidth due to collisions, and possibly a decrease in the biexciton lifetime with increasing density, could cause such a behavior. For the maximum laser intensities at both temperatures ($0.1I_0$ at 5 K and I_0 at 25 K) the calculated biexciton density in the thermal distribution is about 5×10^{18} cm^{-3}. This agrees reasonably well with estimates based on the absorbed laser power, the excited sample volume and a biexciton lifetime of the order of 1 nsec.

Because the measured spectra are time integrated over the duration of the excitation pulse, the biexciton density is not constant. This means, of course, that the chemical potentials must vary during the time of observation, and the values fitted to the data must be regarded as approximate indications of the degree of nonclassical behavior of the biexciton thermal distribution. In any case, it has been found that whenever $|\mu| \lesssim k_BT_{\text{eff}}$, the calculated spectra deviate quite drastically from a classical distribution, and the trend of the data is unambiguous in this respect.

C. Optical probe measurements

One of the distinctive properties of a condensed system of bosons is that if additional particles are

added to the system they will be preferentially attracted into the condensed state, which would normally have negligible statistical weight in the limit of classical behavior. Experiments designed to search for such an effect are very simply devised because of the flexibility of the available methods of optical creation and detection of biexcitons. However, the possible influence of nonlinear optical effects, optical gain, stimulated emission, and particle heating by the optical excitation must be considered carefully in evaluating the results of such measurements.

The experimental approach that has been most successful for biexcitons in CuCl is indicated in Fig. 14, which shows a portion of the exciton and biexciton dispersion curves for small wave vectors. An intense pump beam with a frequency ν_2 tuned to the center of the TPA creates biexcitons at $2\vec{k}_p$. Two, much weaker, counterpropagating probe beams with frequencies $\nu_1=\nu_2+\Delta\nu$ and $\nu_3=\nu_2-\Delta\nu$ create biexcitons only near $\vec{k}=0$ by the simultaneous absorption of one photon from each beam. The magnitude of the detuning $h\Delta\nu$ of the probe beams is 1.64 meV; this is too large compared with the TPA linewidth for any measurable excitation of biexcitons at $2\vec{k}_p$ by either probe beam alone. The probe-induced luminescence in the absence of the pumping at $2\vec{k}_p$ (referred to hereafter as "two-beam spectra") is therefore due to biexcitons scattered from $\vec{k}\sim 0$ into a thermal distribution as was discussed in the preceding section. In order to detect the probe-induced luminescence in the presence of the much stronger emission due to the pump beam (referred to as "three-beam spectra"), the probe beam at frequency ν_3 is mechanically chopped, and the luminescence is synchronously detected using the add-subtract mode of a computer-controlled multichannel analyzer interfaced to the intensified-diode-array detector[43] which was used for these measurements. The luminescence was observed in the nearly backward configuration, relative to the pump beam at ν_2 so that a strong, sharp N_T component was observable in the pump-induced biexciton emission.

Data obtained at a sample temperature of 25 K are shown in Fig. 15. When the pump beam is not present the probe luminescence line shape indicates the expected thermal distribution of biexciton energies (middle trace on the left). In the presence of the pump, the probe emission is strongly redistributed; a sharp line appears at the position of the N_T line, and the decay to the longitudinal branch is sharpened and shifted slightly to higher photon energies (to the left in the figure). The synchronously detected spectrum contains no biexciton emission features whenever either probe beam is blocked. Thus the observed features must be attributed solely to the $\vec{k}=0$ probe excitation. If the intensities of the pump and

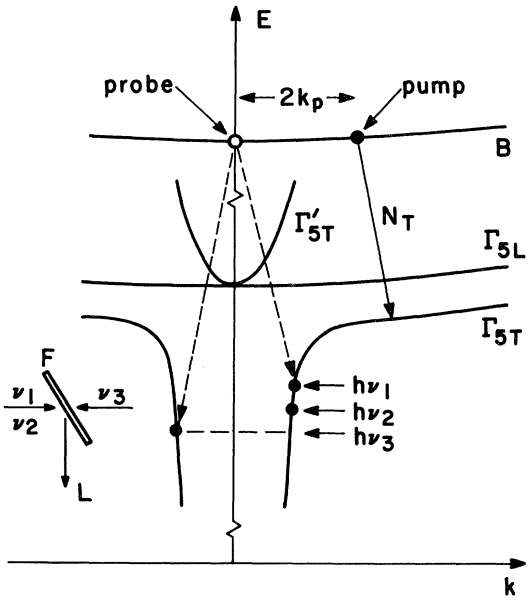

FIG. 14. Schematic exciton and biexciton dispersion curves showing biexciton excitation and radiative decay processes near $\vec{k}=0$. Geometry for the pump and probe experiment is shown in the inset at lower left; ν_1 and ν_3 are the frequencies of the counterpropagating probe laser beams, ν_2 is the intense resonant pump laser beam, L is the detected luminescence in the nearly backward direction relative to the pump beam, and B is the biexciton.

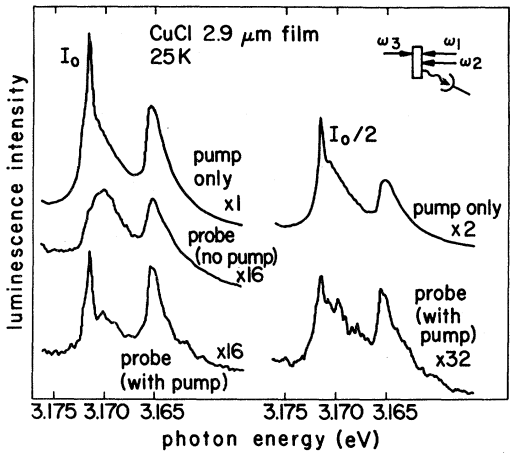

FIG. 15. Biexciton luminescence at $T=25$ K for excitation and detection conditions described in Fig. 17 and the text. Traces labeled probe (no pump) and probe (with pump) were obtained with synchronous detection with the chopping of one of the probe beams.

probe beams are lowered by a factor of 2, the redistribution is still present, but a smaller fraction of the probe emission appears in the N_T line, which is also relatively reduced in the pump-induced luminescence. Because of signal-to-noise limitations it was not possible to extend these measurements to much lower pump intensities without also increasing the ratio of integrated probe emission to integrated pump emission. Spectra analogous to those in Fig. 15, only for a sample temperature of 5 K, were reported previously[44] and will not be repeated here.

We have performed this probe experiment at a number of sample temperatures up to 60 K and over a range of probe emission intensities for a fixed pump intensity. Spectra similar to those in Fig. 15 were obtained at temperatures up to 40 K whenever the integrated probe emission intensity is a few percent or less of the integrated pump intensity. Typical results at several temperatures are shown in Fig. 16. In each case, the integrated probe-induced emission is the same to within the experimental uncertainty, with or without the pump beam. This implies that the observed changes in the chopped component of the luminescence result from a true redistribution of the emission from probe-excited biexcitons, and not from changes in the pump luminescence caused by the presence of the probe excitation.

The character of the three-beam spectra changes markedly when much larger probe excitation intensities are used. This is illustrated in Fig. 17 where the three-beam spectra at $T=5$ K are presented for

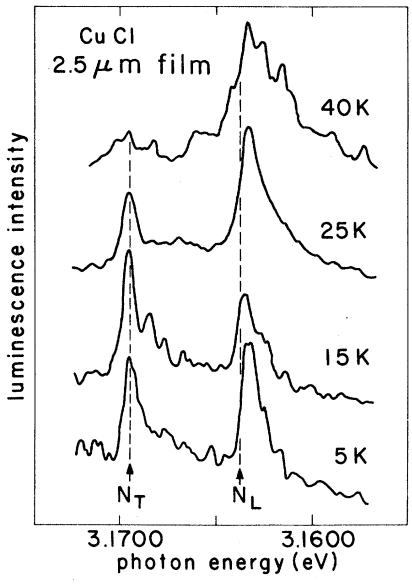

FIG. 16. Probe luminescence in the presence of the resonant pump beam at several sample temperatures.

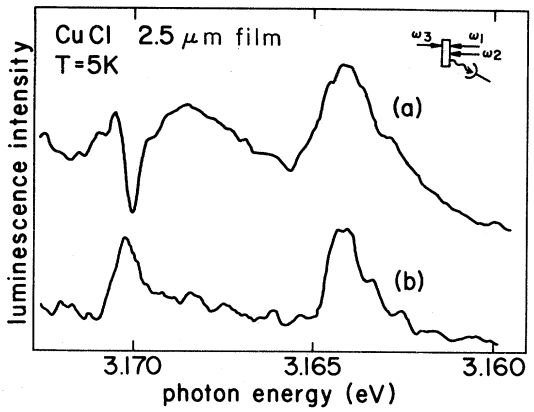

FIG. 17. Chopped-probe-beam luminescence in the presence of the resonant pump beam with $I_0 \sim 1$ MW/cm^2. Intensity of each probe beam in trace (a) is 5 times larger than its intensity in (b).

two different intensities of the probe beam at ν_3 differing by a factor of 5. At the lower intensity, which is similar to that used for the data of Figs. 15 and 16, a peak is observed at the N_T line. At this position in the trace for the higher ν_3 intensity there is, however, a dip corresponding to a reduced, or even negative (phase-reversed), chopped luminescence component. This effect undoubtedly does not result from a decrease in the probe-excited emission at N_T, but from a small reduction of the intense N_T emission line excited by the pump laser. Such behavior is clearly not anticipated for a condensed system of ideal bosons in which all supplementary particles added to the system should be scattered into the condensed state, thereby increasing the N_T emission until, perhaps, the density of $\vec{k}=0$ excited-probe biexcitons becomes comparable to the density at $2\vec{k}_p$.

Although these effects at high-probe-power levels have no conclusive explanation at this time, we have performed another type of probe experiment that yields rather similar results and suggests a possible cause for the high-probe-intensity data of Fig. 17. In this latter experiment, a weak chopped probe beam tuned close to the Z_3 exciton absorption line at about 3.205 eV creates excitons, a fraction of which combine to form biexcitons, although at a somewhat higher effective temperature than in the $\vec{k}=0$ probe experiment. In the presence of resonant pumping of biexcitons at $2\vec{k}_0$, the emission induced by these probe particles is again modified. At the very lowest probe intensities small positive peaks can be observed in the chopped luminescence component, which might be attributed to a quantum attraction of probe particles into the condensate. However, over most of the range of probe intensities the N_T signal is predominantly negative and often

asymmetric, and at large probe intensities it becomes quite large compared with the integrated probe emission measured in the absence of the pump. This signal corresponds, in fact, to a reduction of up to 20% in the N_T component due to the pump excitation. We attribute this to a scattering of the pumped biexcitons away from $2\vec{k}_p$ by the hot injected probe particles. Within the framework of a condensed state at $2\vec{k}_p$, one could account for this behavior on the basis of a heating of the biexciton distribution and a consequent reduction in the condensed fraction of biexcitons. It is apparent from the fits to the data of Figs. 10 and 11 that the effective particle temperature also increases with increasing resonant excitation. This effect could possibly account for the dips observed at higher probe powers in Fig. 17, and the observed asymmetries in the N_T signal could be due to a very slight shift of the TPA resonance by the local heating of the sample.

The simplest explanation of the three-beam data of Figs. 15 and 16 is the attraction of the probe particles into the $2\vec{k}_0$ pumped state via interparticle collisions or phonons. Nevertheless, some test experiments have been performed in order to examine the possibility that optical gain and stimulated emission are the cause of the luminescence redistribution. For highly excited optical systems, these two processes are related, but not necessarily in a simple way because of several complex factors; a few of these factors are gain saturation, geometrical effects, and density-dependent collision rates and quantum efficiencies. We have therefore examined these two possibilities separately.

The optical gain caused by the pump excitation was measured directly with a chopped, broadband probe beam produced by emission from a dye cell. This cell is pumped by the same N_2 laser that excites the dye laser used for the resonant pump beam. The pump and probe beams were counterpropagating, so that the gain in the direction of the backward emission is measured. In that direction, which is nearly identical to the direction of the emission observed in Figs. 15–17, the N_T emission has a maximum intensity and N_L is forbidden.

Typical data obtained at several sample temperatures are shown in Fig. 18, where the pump intensity I_0 is the same as that used in the probe experiments. Similar data were obtained over a large range of temperatures and probe intensities.[17] For the data of Fig. 18 the probe intensity within the bandwidth of the N_T line is comparable to the N_T emission excited by the pump, and the gain of 23% at the N_T position at $T=5$ K is the largest that we have measured. It decreases somewhat at lower probe intensities and is considerably smaller at higher temperatures. For example, the gain measured for the N_T line under the conditions of the higher pump power of Fig. 11 is 10% over the full thickness of the film. The probe emission travels, on the average, half the thickness of the excited region, so the probe amplification would be even smaller. We conclude that the effects of amplification of the probe emission would be to cause a very small N_T peak in the three-beam spectra, but it could not account for the much more extensive redistribution of the emission evident in Figs. 15 and 16. Amplification would also not conserve the integrated probe emission since some of the chopped luminescence intensity would be supplied by the pump beam through its amplification of the probe emission.

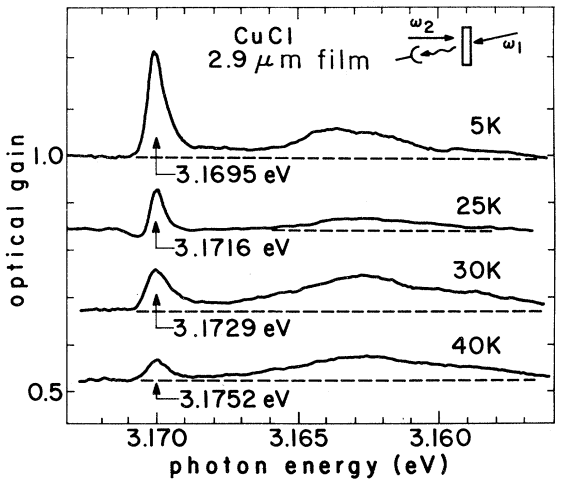

FIG. 18. Optical gain of a broadband probe beam propagating in the backward direction relative to a resonant pump beam with intensity $I_0 \sim 1$ MW/cm^2. Gain scale on the left and photon energy scale are appropriate to the $T=5$ K trace. Traces for other temperatures have been shifted along the horizontal axis to align the N_T components, and along the vertical direction to avoid overlap. Dashed line in each trace corresponds to a gain of unity (no net amplification).

Stimulated emission of the probe biexcitons caused by the more intense pump-induced luminescence could, in principle, account for the luminescence redistribution. However, the nearly two-dimensional excitation geometry in these films would favor stimulation in the plane of the film where the excitation length of several tens of micrometers would lead to a more rapid growth of photon flux than in the direction normal to the film. Since probe photons emitted in the plane of the film would not be directly observable in our nearly backward experimental geometry, this stimulated emission mechanism would also not conserve the integrated probe emission intensity. Furthermore, be-

cause of the polariton dispersion, N_T emission in the plane of the film occurs at a photon energy about 0.5 meV higher than in the backward direction. While a weak shoulder is often observed in our emission data at such an energy, it accounts for only a small fraction of the N_T component in the three-beam and pump luminescence data.

Experimental verification that stimulated emission cannot account for the redistribution of probe luminescence has been obtained in a variation of the probe experiment in which a pump beam is tuned not to the biexciton TPA but to the wavelength region of the biexciton emission. In this way, any stimulated emission of probe biexcitons caused by pump photons can be examined without the presence of any biexcitons created by the pump. The two-beam and three-beam probe emission obtained in such an experiment at $T=5$ K with the unchopped pump laser tuned to the N_T emission line are shown in Fig. 19. In this case, the pump intensity is about an order of magnitude larger than the N_T emission observed with resonant pumping. In the three-beam trace only some residual noise due to the pump laser is observed at the position of the N_T line, and there is no detectable redistribution of the probe emission. This shows that the stimulation effect is not the cause of the N_T feature or of the luminescence redistribution in Figs. 15. and 16.

V. DISCUSSION

The development of a quasistable condensed state in a system of excitonic particles is contingent on the production of an appropriately large particle density and the existence of thermal-relaxation processes that are rapid enough to achieve a thermal equilibrium distribution of particle energies on a time scale substantially shorter than the particle lifetime. The possibility of achieving these conditions for biexcitons in CuCl, and the characteristics of the condensed state, depend not only on the properties of the biexciton itself, but they may also be influenced by the existence of stimulated emission and the coherent mode of creation of the biexcitons with resonant laser excitation. These factors are discussed below in light of the current knowledge of the properties of biexcitons and excitons in CuCl.

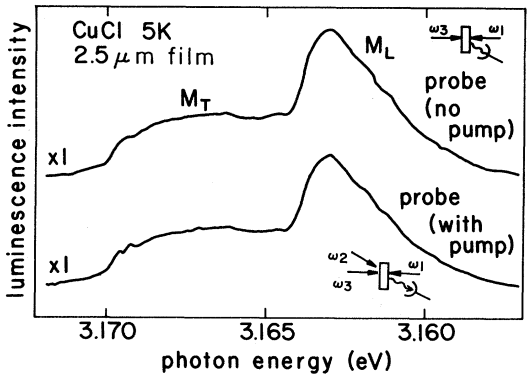

FIG. 19. Chopped-probe luminescence at a sample temperature of 5 K. In the lower trace, a pump laser beam with an intensity about an order of magnitude greater than the detected N_T luminescence is present at the N_T frequency.

A. Biexciton density

For resonant two-photon excitation at $2\vec{k}_p$, the biexciton density ρ_B can be estimated from the relation $\rho_B=\eta I_l \tau_B/E_m d$, where I_l is the laser intensity, η is the fraction of laser power absorbed in a thickness d of the sample, τ_B is the biexciton lifetime, and $E_m=6.372$ eV is the biexciton energy at $\vec{k}\sim 0$. The primary cause of uncertainty in making such an estimate is the large variation in the lifetime τ_B obtained from the various experiments that have been reported. The main factors which might cause such variations are a density-dependent decay rate due to stimulated emission, Auger decay, or reformation of biexcitons from excitonic decay products and a possibly sample-dependent nonradiative decay due to defects or surfaces.

The longest reported biexciton lifetime of about 3×10^{-9} sec was obtained by monitoring the luminescence decay at a low biexciton density in bulk single crystals.[45] Lifetimes of $(2-3)\times 10^{-10}$ sec have been measured from the luminescence decay using resonant excitation with very intense ($\gtrsim 10$ MW/cm^2) picosecond sources in bulk CuCl (Ref. 46) and thin platelet samples.[47] An intermediate value for τ_B of about 10^{-9} sec has been obtained from induced absorption measurements fitted with a model using exciton and biexciton decay rates and the recombination of excitons to form biexcitons.[48] The 4.5×10^{-9}-sec-long excitation pulses used in the present experiments were not suitable for a lifetime measurement in the evaporated-film samples. However, the luminescence quantum efficiency of the films was quite similar to that of single-crystal CuCl platelets and bulk samples measured under very similar conditions. It is therefore reasonable to take a value $\tau_B=10^{-9}$ sec for the purposes of estimating the biexciton density for excitation conditions such that there are no noticeable indications of stimulated emission in the biexciton luminescence. At an intensity $I_l\sim 1$ MW/cm^2, the absorbed fraction measured in experiments similar to those in Fig. 4 with $d\sim 10^{-4}$ cm is $\eta\sim 0.25$. The estimated biexciton density is $\rho_B=2.5\times 10^{18}$ cm^3. The condensation temperature at this density is about 11 K. Consider-

ing the uncertainties in estimating the biexciton lifetime and the laser intensity, which is a temporal and spatial average over the 5×10^{-9}-sec pulse width and over the focal region, this value of T_c is in reasonable agreement with the experimental results, which indicate the presence of a condensed state at temperatures up to 40 K at laser intensity levels of several MW/cm^2.

B. Thermal relaxation

Interparticle collisions and interactions with phonons both play a role in establishing the kinetic energy distribution of the biexcitons. At the highest biexciton densities produced in the present work, mean collision times on the order of a picosecond may be inferred from either the impact-parameter model[46] or from the "cage" model, which is probably more appropriate to the highest densities encountered in these experiments.[30] Since the biexciton lifetime and the exciting laser-pulse width are 2—3 orders of magnitude longer, a quasiequilibrium thermal distribution of particle energies exists even without complete thermalization with respect to the lattice, so that the effective temperature of this distribution is higher than that of the lattice. The fits to the luminescence data of Figs. 10—13 suggest that this is the case for lattice temperatures below 15—20 K. The effective particle temperatures also depend strongly on excitation level at these lower temperatures.

At lattice temperatures above 20 K, the fitted particle temperatures tend to follow closely the lattice temperature, which suggests that the rate of equilibration with the lattice becomes comparable to the biexciton decay rate. Similar conclusions have been made from recent measurements of the luminescence line shapes in single-crystal platelets of CuCl.[33]

On the leading edge of the excitation light pulse, the thermal distribution must build up from the excitation near $\vec{k}=0$. The additional energy required to scatter the resonantly created biexcitons into the states of much higher wave vectors in the thermal distribution must come from collisions with biexciton decay products or phonons. Observations of the time dependence of the N_T line and the broad M_T and M_L bands were performed in the course of this investigation. There was no noticeable difference between them on a time scale of about 10^{-9} sec, which is the limit of the time resolution of the photomultiplier tube and electronics. This result implies that the buildup of the thermal biexciton distribution occurs on a time scale that is short compared to the laser excitation pulse, and the narrow and broad luminescence components are emitted simultaneously. In summary, it is apparent that relaxation processes, particularly collisions, are sufficiently rapid to allow a quasiequilibrium to develop for nearly all of the duration of the laser excitation pulse.

C. Stimulated emission

A thorough treatment of stimulated emission for the case of biexcitons is clearly beyond the scope of this discussion; the anisotropy of the emission, the dependence of emission frequency on exciton wave vector, the longitudinal-transverse exciton splitting, and the geometry of the sample and excitation conditions lead to a very complex problem in the most general case. It is, however, possible to make some rough estimates of the effects of stimulated emission in order to verify that it is not the cause of the experimental results that are attributed to the existence of a condensed state of biexcitons, and that it does not seriously affect the biexciton lifetime at the power densities used in this investigation.

The simplest approach to the problem is to write the radiative transition rate in terms of the spontaneous emission lifetime t_s, a normalized shape function $g(\nu)$, and the average biexciton emission intensity I_e, in the excited region of the sample,[49]

$$W=\frac{\lambda^2 I_e g(\nu)}{8\pi h\nu n^2 t_s}\ . \tag{10}$$

In this expression, $n=2.75$ is the refractive index of CuCl, λ is the wavelength, and ν is the frequency of the emission. Strictly speaking, I_e is the single-mode light intensity, but it will be taken here to be the total intensity since the total stimulated emission rate is the sum over all radiation modes in the absence of saturation effects. In order to obtain the absolute maximum stimulated emission rate we assume that all of the absorbed laser power is reemitted by biexcitons, so that $I_e=\eta I_0\sim2.5\times10^5$ W/cm^2. This is equivalent to assuming a unit quantum efficiency for the biexciton emission so that t_s is the biexciton lifetime, $t_s\sim10^{-9}$ sec. An average value of $g(\nu)\sim10^{-12}$ sec at the peak of the N_T line is estimated from the frequency distribution of the luminescence in Figs. 2—4. The resulting stimulated emission rate is $W=5\times10^9$ sec^{-1}. This is a factor of 5 larger than the assumed spontaneous decay rate t_s^{-1} which suggests that stimulated emission could be a factor in reducing the biexciton lifetime and distorting the luminescence distribution, but only at the highest excitation intensities.

The unsaturated optical gain coefficient at the peak of the N_T or N_L line may be estimated in a similar fashion from the expression[49]

$$\gamma=\frac{N_B\lambda^2 g(\nu)}{8\pi n^2 t_s}\ , \tag{11}$$

where N_B is the number of biexcitons at $\vec{k}=2\vec{k}_p$. It is assumed for this estimate that the exciton population in the terminal states of the N_T emission is negligible; the effect of this assumption is to overestimate the gain coefficient. In this case, the appropriate $g(\nu)\sim 5\times 10^{-12}$ sec is estimated from the calculated width of the emission in the N_T line, which is broadened not only by the anisotropic emission frequency, but by biexciton and exciton collisions, and inhomogeneous broadening. For a biexciton density at $\vec{k}=2\vec{k}_p$ of 10^{18} cm^{-3}, as would be the case if about 10–40% or so of the biexcitons were emitting from $2\vec{k}_p$, we obtain $\gamma\sim 4\times 10^4$ cm^{-1}. The measured optical gain in Fig. 16 is given by $\exp(\gamma t)$, where t is the thickness of the excited region of the sample. The maximum measured gain of 1.23 corresponds to $\gamma\cong 0.2\times 10^4$ cm^{-1}, a factor of 20 smaller than the estimate from Eq. (11), assuming $t\sim 1$ μm for the effective excitation length.

It is possible that this difference is partly the result of gain saturation due to a buildup of the population of excitons in the terminal states for the N_T emission. However, it is also likely that the radiative quantum efficiency of the biexciton is considerably less than unity, possibly as low as 10%. This statement is based on a comparison between the integrated intensity of the detected luminescence, corrected for the total detection efficiency, and the absorbed laser light at the peak of the TPA. In that event, the spontaneous radiative decay time t_s may be longer than the 10^{-9} sec that we have assumed, and the emission intensity I_e would be lower. As a result, the estimated gain coefficient would be closer to the rather small measured value, and the stimulated emission rate, which is proportional both to I_e and t_s^{-1}, would be considerably reduced. This is consistent with the observations that evidence of stimulated emission is found at laser intensities above 5–10 MW/cm^2, considerably larger than those used for most of the experimental results reported here. Stimulated emission should first occur in or near the plane of the film because the dimension of the excited region is largest there. The angular dependence of N_L and N_T emission given in Eqs. (5a) and (5b) show that the N_T emission is slightly more intense than N_L at 90° to the excitation laser beam. However, scattering processes rapidly deplete the population of the longitudinal exciton branch at temperatures below about 50 K, so that the gain of the N_L component will not saturate as quickly as that of N_T.[14] This undoubtedly explains the sudden appearance of a stimulated N_L Raman component in Fig. 12 at very high power levels, whereas no N_T component is visible.

Of most importance to the question of the existence of a condensed state of biexcitons is the fact that these estimates of stimulated emission rates lend support to the experimental evidence that the luminescence redistribution at high densities and low temperatures is not simply the result of stimulated emission. For this to be true, the stimulated emission rate must be comparable to the collision rate so that a large fraction of the biexcitons injected at $\vec{k}=0$ or $\vec{k}=2\vec{k}_p$ decay radiatively before being scattered into the thermal distribution. This would require an emission rate from $2\vec{k}_p$ alone approaching 10^{11}–10^{12} sec^{-1}, about 2 orders of magnitude larger than the estimate from Eq. (10).

D. Effects of the resonant excitation

The presence of anisotropic sharp lines with $\vec{k}=2\vec{k}_p$ excitation, and the lack of such features with $\vec{k}=0$ excitation can be accounted for on the basis of a Bose-Einstein–condensed state only if the wave vector of the condensate is the same as that of the state populated by the laser pumping. There are several reasons why this situation is likely. With $\vec{k}=0$ excitation no net momentum is transferred to the biexcitons, whereas with the single-beam geometry a momentum of $2\vec{k}_p$ per particle is imparted by the excitation process. The energy separation between $\vec{k}=0$ and $\vec{k}=2\vec{k}_p$ is about 15 μV, several orders of magnitude smaller than $k_B T_{\text{eff}}$ for the biexcitons. The excess energy associated with a condensed state at $\vec{k}=2\vec{k}_p$ is therefore negligible. The direct relaxation between $2\vec{k}_p$ and $\vec{k}=0$ states by the emission of an acoustic phonon is not possible because the biexciton and acoustic-phonon dispersion curves intersect only at a wave vector $q\sim 3.5\times 10^6$ cm^{-1}; this is about an order of magnitude larger than $2\vec{k}_p$. Higher-order processes, involving multiple phonons, or phonons plus particle collisions, are required for lattice-induced relaxation of a condensate at such a small wave vector. It is therefore not unreasonable that a condensate at a small, finite wave vector should be stable for time intervals on the order of the 10^{-9}-sec biexciton lifetime.

The presence of the laser pumping of biexcitons into a state of nonzero wave vector leads to a steady-state population there that is far above the thermal-occupation level even in the presence of the large scattering rates of about 10^{12} sec^{-1} inferred from the broadening of the TPA. This laser-induced coherence may serve to nucleate a condensation at the pumping wave vector[21] since the time of formation of the BEC should be considerably shortened by stimulated scattering of particles into the

pumped state. This possibility leads naturally to the question of whether the energy of the condensed state can also be selected by the laser excitation. Experimentally, such a situation may result in a shift of the narrow emission components as the laser frequency is varied. It is not clear at this time whether the small shifts in the N_T emission shown in Figs. 6 and 7 or the hyper-Raman effects observed at higher laser intensities could be manifestations of such an effect. Optical probe measurements like those in Sec. IV C as a function of excitation wavelength may provide evidence regarding this question.

VI. CONCLUSIONS

Several features of the optical properties of biexcitons in CuCl can be explained in a direct way if it is assumed that a Bose-Einstein—condensed state exists at high biexciton densities and at sample temperatures as high as 40 K. Two experimental results give the most direct support for this conclusion. First, nonclassical energy distributions of the biexcitons have been observed which can be well fitted in the framework of the ideal-Bose-gas model. Values of the chemical potential that go to zero at the highest densities are deduced from a line-shape analysis of the biexciton luminescence. Furthermore, the expected trend is observed, namely, a gradual evolution towards a classical statistical regime if the particle density is decreased or if the lattice temperature is increased. Second, a redistribution of injected probe particles is observed, which verifies the property of quantum attraction of particles into the condensed state. Other features of the biexciton emission that are also consistent with these conclusions are the appearance of sharp, anisotropic, and polarized emission lines at high excitation levels and low temperatures. In addition, the available evidence concerning particle densities, effective temperatures, and collision rates implies that the requirements necessary for the existence of BEC are satisfied for the conditions of resonant excitation used in this work.

ACKNOWLEDGMENTS

The authors are grateful to M. Combescot, G. Grynberg, G. D. Mahan, and P. Tua for very helpful conversations and theoretical enlightenment. This work was supported by National Science Foundation under Grants Nos. DMR-78-09426 and DMR-81-05005, Centre National de la Recherche Scientifique, France, and NATO Grant No. 1483.

---

*Present address: Optical Sciences Center, University of Arizona, Tucson, AZ 85721.

[1]The properties of biexcitons have been reviewed in E. Hanamura and H. Haug, Phys. Rep. 33, 209 (1977); C. Klingshirn and H. Haug, *ibid.* 70, 315 (1981).

[2]E. Hanamura, Solid State Commun. 12, 951 (1973).

[3]M. I. Sheboul and W. Ekardt, Phys. Status Solidi B 73, 165 (1976).

[4]T. Mita, K. Sôtome, and M. Ueta, Solid State Commun. 33, 1135 (1980).

[5]F. London, *Superfluids* (Wiley, New York, 1945), Vol. 2, p. 43.

[6]M. Inoue and E. Hanamura, J. Phys. Soc. Jpn. 41, 771 (1976).

[7]Y. Yakhot and E. Levich, Phys. Lett. 80A, 301 (1980).

[8]S. Shionoya, in *Proceedings of the 12th International Conference on Physics of Semiconductors, Stuttgart,* edited by M. H. Pilkuhn (Teubner, Stuttgart, 1974), p. 113.

[9]N. Nagasawa, N. Nakata, Y. Doi, and M. Ueta, J. Phys. Soc. Jpn. 39, 987 (1975).

[10]N. Nagasawa, T. Mita, and M. Ueta, J. Phys. Soc. Jpn. 41, 929 (1976).

[11]R. Levy, C. Klingshirn, E. Ostertag, V. Duy Phach, and J. B. Grun, Phys. Status Solidi B 77, 381 (1976).

[12]E. Ostertag, A. Bivas, and J. B. Grun, Phys. Status Solidi B 84, 673 (1977).

[13]B. Hönerlage, V. Duy Phach, and J. B. Grun, Phys. Status Solidi B 88, 545 (1978).

[14]E. Ostertag, R. Levy, and J. B. Grun, Phys. Status Solidi B 69, 629 (1975).

[15]R. Levy, R. Hönerlage, and J. B. Grun, Phys. Rev. B 19, 2326 (1979).

[16]M. Ojima, Y. Oka, T. Kushida, and S. Shionoya, Solid State Commun. 24, 845 (1977).

[17]N. Peyghambarian and L. L. Chase (unpublished).

[18]K. L. Shaklee, R. F. Leheny, and R. E. Nahory, Phys. Rev. Lett. 26, 888 (1971).

[19]J. H. Hvam and A. Bivas, Phys. Status Solidi B 101, 363 (1980).

[20]L. L. Chase, N. Peyghambarian, G. Grynberg, and A. Mysyrowicz, Phys. Rev. Lett. 42, 1231 (1979).

[21]K. Sôtome, Y. Nozue, and M. Ueta, Solid State Commun. 36, 555 (1980).

[22]T. Kushida, Solid State Commun. 36, 555 (1980).

[23]T. Itoh, S. Watanabe, and M. Ueta, J. Phys. Soc. Jpn. 48, 542 (1980).

[24]T. Hansch, Appl. Opt. 11, 895 (1972).

[25]A. J. Schmidt, Opt. Commun. 14, 294 (1975).

[26]F. Bassani, J. J. Forney, and A. Quattropani, Phys. Status Solidi B 65, 591 (1974).

[27]B. Hönerlage, A. Bivas, and Vu Duy Phach, Phys. Rev. Lett. 41, 49 (1978).

[28]T. Mita, K. Sôtome, and M. Ueta, Solid State Commun.

33, 1135 (1980).
[29]G. M. Gale and A. Mysyrowicz, Phys. Rev. Lett. 32, 727 (1974).
[30]L. L. Chase, N. Peyghambarian, G. Grynberg, and A. Mysyrowicz, Opt. Commun. 28, 189 (1979).
[31]L. L. Chase, G. Grynberg, and A. Mysyrowicz, Opt. Soc. Am. 68, 678 (1978).
[32]M. Kuwata, T. Mita, and N. Nagasawa, Opt. Commun. 40, 208 (1981).
[33]T. Itoh, S. Watanabe, and M. Ueta, J. Phys. Soc. Jpn. 48, 542 (1980).
[34]T. Itoh and T. Kathono, J. Phys. Soc. Jpn. 51, 707 (1982).
[35]N. Peyghambarian, L. L. Chase, and A. Mysyrowicz, Opt. Commun. 42, 51 (1982).
[36]M. Kuwata, T. Mita, and N. Nagasawa, J. Phys. Soc. Jpn. 50, 2467 (1981).
[37]S. Schmitt-Rink and H. Haug, Phys. Status Solidi B 108, 377 (1981).
[38]F. Henneberger, K. Henneberger, and J. Voigt, Phys. Status Solidi B 83, 439 (1977).
[39]J. J. Hopfield, Phys. Rev. 112, 1555 (1958).
[40]R. Levy, C. Klingshirn, E. Ostertag, Vu Duy Phach, and J. B. Grun, Phys. Status Solidi B 77, 381 (1976).
[41]M. Ojima, T. Kushida, S. Shionoya, Y. Tanaka, and Y. Oka, J. Phys. Soc. Jpn. 45, 884 (1978).
[42]A. Bivas, Vu Duy Phach, B. Hönerlage, and J. B. Grun, Phys. Status Solidi B 84, 235 (1977).
[43]Tracor Northern model TN-1710 with intensified TN-1223 diode-array detector.
[44]N. Peyghambarian, L. L. Chase, and A. Mysyrowicz, Opt. Commun. 41, 178 (1982).
[45]G. M. Gale and A. Mysyrowicz, Phys. Lett. 54A, 321 (1975).
[46]M. Ojima, T. Kushida, Y. Tanaka, and S. Shionoya, J. Phys. Soc. Jpn. 44, 1294 (1978).
[47]Y. Segawa, Y. Aoyagi, O. Nakagawa, K. Azuma, and S. Namba, Solid State Commun. 27, 785 (1978).
[48]E. Ostertag and J. B. Grun, Phys. Status Solidi B 82, 335 (1977); R. Levy, B. Hönerlage, and J. B. Grun, Phys. Rev. B 19, 2326 (1979).
[49]Amnon Yariv, *Quantum Electronics,* 2nd ed. (Wiley, New York, 1975), pp. 161—162.